

See discussions, stats, and author profiles for this publication at: <https://www.researchgate.net/publication/366572474>

Portable Drilling Machine Applied as a Friction Stir Tool to Join Light Metals

Article in Applied Engineering Letters Journal of Engineering and Applied Sciences · December 2022

DOI: 10.18485/aeletters.2022.7.4.3

CITATIONS

0

READS

48

3 authors:



Ahmad K Jassim
University of Basrah

36 PUBLICATIONS 257 CITATIONS

[SEE PROFILE](#)



Raheem Al-Sabur
University of Basrah

32 PUBLICATIONS 108 CITATIONS

[SEE PROFILE](#)



Dhia Ali
University of Basrah

4 PUBLICATIONS 4 CITATIONS

[SEE PROFILE](#)

Some of the authors of this publication are also working on these related projects:



Call for Papers (Sustainable Polymer Composites using Machine Learning) [View project](#)



Friction Stir Coating process [View project](#)

PORTABLE DRILLING MACHINE APPLIED AS A FRICTION STIR TOOL TO JOIN LIGHT METALS

Original scientific paper

UDC:621.791.763
<https://doi.org/10.18485/aeletters.2022.7.4.3>Ahmad K. Jassim¹, Raheem Al-Subar^{2*}, Dhia Ch. Ali³¹Research & Development Department, The State Company for Iron and Steel, Basrah, Iraq²Mechanical Department, Engineering College, University of Basrah, Basrah, Iraq³Materials Department, Engineering College, University of Basrah, Basrah, Iraq

Abstract:

Sustainable manufacturing technology is one of the requirements of the current industrial fields to reduce the weight and energy used. Friction stir welding (FSW) can be considered a quantum leap in the development of welding technology. A solid-state process utilizes a non-consumable tool and less electrical energy. Friction stir spot welding (FSSW) is a particular case of FSW that began to spread rapidly, especially for similar and dissimilar metals, which has extended to weld the polymers. The increase of FSSW use in different fields needs to simplify the equipment. This study used a portable drilling machine to construct an FSSW apparatus with a rotational speed between 1500 and 3000 rpm with a pin diameter of 2, 3 and 4 mm. The results indicated that the joints welded by the developed apparatus have good strength and hardness. Furthermore, many specimens succeeded in the bending test, especially when the rotational speed was set at 2250 rpm and the pin diameter was 3 mm. In addition, it was found that the mechanical properties increased with the rotational speed and pin diameter, then gradually decreased. Finally, the Response Surface Methodology (RSM), besides the analysis of variation (ANOVA), was utilized to maximize the lap-shear fracture load. The results indicated that the maximum lap-shear fracture load can be achieved at a tool speed N of $\{2300 > N > 1600\}$ rpm with a pin diameter (d) of $\{2.75 > N > 3.75\}$ mm.

ARTICLE HISTORY

Received: 03.10.2022.

Accepted: 21.12.2022.

Available: 31.12.2022.

KEYWORDS

FSSW, friction stir spot welding, drilling machine, FSW, response surface methodology, light metals

1. INTRODUCTION

FSSW is a solid-state welding process for joining lightweight metals like aluminium alloys. A non-consumable tool used to joint two plates through friction and plastic deformation. The process is done by plunging a rotating pin that uses frictional heat and mechanical work to connect between sheets that overlap [1].

The FSW method was invented by the Welding Institute (TWI) in the early 1990s [2, 3]. It is a relatively new discrete process derived from FSW. It is a relatively new discrete process that has been used in several automobiles, where it can save

about 90% of energy consumption compared to conventional resistance spot welding (RSW) [4, 5]. The main reason to apply FSSW instead of RSW is to reduce joining defects, including significant heat distortion and high-power consumption. FSSW has been used successfully on aluminium alloys, magnesium, copper and steel, which has been used in transportation to save weight [6, 7]. FSSW is an excellent way to fix the problems of traditional fusion welding, such as porosity, cracks and oxide inclusions and residual stresses [8]. The mechanical properties and joint quality are affected by several parameters, including the tool's geometry, plunge rate, rotating speed, and dwell duration [9].

In the FSSW, two plates are joined in the configuration lap. The rotational tool is characterized by a cylindrical part of a large diameter called the shoulder, followed by a small diameter part called the pin. The FSSW includes three stages: plunging, stirring and drawing. A milling or drilling machine is used to rotate the tool at the required speed and then take a downward motion until the pin reaches the top layer of the upper plate. The pin threads into the first plate and pierces it until it penetrates the lower plate. In the meantime, the shoulder face becomes in direct contact with the upper plate for a certain period called "dwelling time", and sufficient heat is generated to link the two pieces. Then the tool is withdrawn and leaves the area to cool, as indicated in Fig. 1 [10].

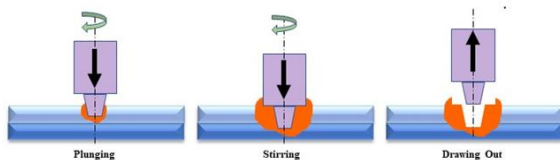


Fig. 1. Stages of the FSSW process [11]

AA6061 is one of the most widely used aluminium alloys due to its high corrosion resistance, even in harsh environments like seawater. Therefore, it is used in the FSW process to improve the strength from medium to high with good hardness properties. In terms of heat treatments, this alloy is one of the most versatile alloys, and when appearance is important, it meets ambitions, so it is widely used and has many industrial applications.

Merzoug et al. [12] reported that the FSSW parameters greatly influenced the mechanical properties. The results indicated that when the tool speed was doubled, the tension-shear strength was reduced by 38%, while the dwell time did not exceed a specific value. Shen et al. [13] studied the welding parameters effect on the joint microstructure using a concave profile shoulder. When the dwell time and tool speed were improved, the minimum resulting hardness was achieved at the heat-affected zone (HAZ) and thermo-mechanically affected zone (TMAZ). Sato et al. [14] examined the material flow during the FSSW. The results indicated a spiral flow along the pin and then released at its end.

FSSW can be considered an environmentally friendliness process with no noise or spatters and low vapour emissions and consumables as the main advantages of this process. On the other hand, one of the main disadvantages of FSSW is that the

nugget of the welding includes a desirable hole in its centre which may cause corrosion later [15]. Several studies tried to overcome the hole problems by using a pinless tool [16], a refill FSSW process [17] and a double-side FSSW [18, 19].

Pandey and Mahapatra used optical microscopy to ensure that the pressure produced by the rotating tool pushes the material from the upper plate to flow plastically to the lower plate. The components are combined in a plastic manner to create the weld for aluminum 6061 [20]. Pinless FSSW can achieve a tensile shear of 52.9% of the conventional FSSW besides overcoming the keyhole for the AA 6061-T6 aluminum alloy [21]. Furthermore, the pinless tool was used to join dissimilar alloys, such as AA6061 aluminum and DP600 steel sheets, to study the failure load and microstructure. The study showed that a maximum failure load of 4.4 kN could be reached with an axial load of 16 kN, a rotational speed of 1300 rpm, and a dwell time of 10 s [22].

RSM is characterized as mathematical and statistical among several optimization algorithms. Despite the first use of the method in the 1950s, it is still an active method in many experimental studies, especially in FSW and FSSW [23]. In RSM, the input variables are called independent parameters, while the outputs are called process responses.

The RSM method for optimization has three crucial steps: statistically designed experiments, calculating the mathematical model coefficients, predicting the response, and verifying the model's fit within the experiment setup [24, 25].

The governing equation of the RSM is described below [23]:

$$Y = \Phi(x_1, x_2, \dots, x_k) \pm e_r \quad (1)$$

$$Y = b_0 + \sum b_i x_i + \sum b_{ij} x_i^2 + \sum b_{ij} x_i x_j + e \quad (2)$$

Where b_0 , b_i , and b_{ij} are constant, linear and quadratic coefficients to estimate the output response Y .

The increasing of using FSW and FSSW in many new fields, such as joining polymers and composites [26], underwater welding [27], and battery trays [28], must result in the simplification and expansion of FSSW equipment manufacturing. This article tries to apply domestic drilling machines to be part of the FSSW apparatus.

When reviewing the FSSW literature, it can be noted that there are no attempts to make this welding portable, and it can be used as a domestic

tool for welding sheets of light metals and polymers. The suggested apparatus is a portable FSSW tool accessible for construction and has a low cost. The mechanical properties of the joints were examined using a tensile lap shear test, a hardness test, and a bending test. Finally, the RSM was used to examine the optimum welding parameters.

2. MATERIALS AND METHODS

The COOFIX CF-ED003 portable drilling machine was prepared as a rotational tool during of FSSW process. At no load, the selected drilling machine has a tool speed of 3300 rpm with a drilling capacity of 10 mm, which needs 450 Watts. The drilling machine was set up inside a sliding stand where its movement was done by a manual rod. Iron support was added, which included a hole to fix the two sheets that needed to be joined and a passageway for the drill tool to join the sheets, as shown in Fig. 2-a. The whole system was firmly fixed on a wooden base by bolts. Finally, the regular beat tool in the drill chuck was replaced by specific dimensions tool.

The modified tool is made of tungsten carbide, which consists of a long cylindrical part called the shoulder, whose diameter has been reduced to form a pin or probe, as shown in Fig. 2-b. This study used three tool diameters of 2, 3 and 5 mm, while the shoulder remained at the same diameter of 10 mm. The overall dimension of the apparatus is 15x20x32 cm.

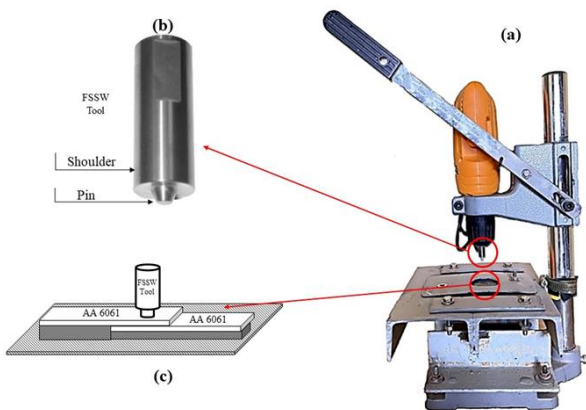


Fig. 2. The FSSW apparatus (a) main apparatus, (b) FSSW tool, (c) specimens' arrangement

Aluminium AA6061 alloy sheets were firmly fixed as a lap joint in the FSSW apparatus, as shown in Fig. 2-c. An anvil and a supporter were used to stem the movement of the sheets. The chemical composition of the AA6061 is indicated in Table 1.

A tool made of high-chromium high-carbon steel (HCHCR-D2) was used. The tool chemical composition is shown in Table 2.

Table 1. AA 6061 chemical compositions [Measured]

Material	%
Cu	0.6
Fe	0.39
Si	1.0
Mg	1.2
Mn	0.2
Cr	0.28
Ti	0.15
Zn	0.28
Al	Bal

Table 2. FSSW tool chemical compositions [Measured]

Cr	S max	Si	Mn	P max	C
11.51	0.03	0.39	0.38	0.03	2.14

All the sheets were cut off into rectangular shapes of 3 x 25 x 100 mm, and every two sheets were fixed as indicated on the apparatus bench. Fig. 3 shows the preparation of the overlap specimens for the FSSW process according to the American Welding Society.

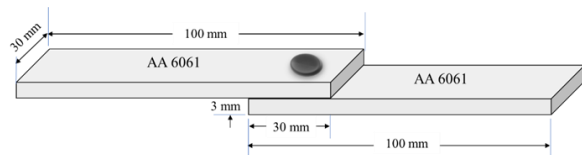


Fig. 3. AA6061 specimens' dimensions

During the experimental work, the rotational speed and pin diameter were considered the essential process parameters for optimizing the lap-shear fracture load during the FSSW. The rotational speeds used in this research include 1500, 2250, and 3000 rpm, while selected pin diameters are 2, 3, and 4 mm. The drill has four speeds which can be changed manually by using a small rolling wheel that is present in the drill. The axial pressures applied for welding were done using a manual hand arm. The first needs high pressure and then low pressure when the heat is generated by friction. The required load decreases with an increasing fraction of heat generated during the welding process. The Instron universal tensile machine (Instron, USA) was used to get the lap-shear fracture load according to ASTM D1002. The average of the two samples was dependent, and the resulting shear load with corresponding process parameters is shown in Table 3.

Table 3. The lap-shear fracture load values during the FSSW process

Rotation speed (rpm)	Pin diameter (mm)	Lap-shear fracture load(N)
1500	2	599
1500	3	750
1500	4	671
2250	2	622
2250	3	840
2250	4	711
3000	2	301
3000	3	559
3000	4	433

3. RESULTS AND DISCUSSION

3.1 lap-shear fracture load Analysis

RSM was used to achieve the maximum lap-shear fracture load based on Minitab 19 software. The central composite design (CCD) of two factors and three-level was utilized in RSM to investigate nine experimental works. According to the analysis of variation (ANOVA) shown in Table 4, the rotational speed significantly affects welding lap-shear fracture load. The F-value of rotational speed is 119, which is five times the influence of the pin diameter 19. Fig. 4 indicates the average lap-shear fracture load variation using the developed FSSW apparatus concerning welding parameters. For both rotational speed and pin diameter, the obtained lap-shear fracture load increases gradually with both and then goes down gradually. The maximum lap-shear fracture load value is 840N, achieved at a rotational speed of 2250 rpm and a pin diameter of 3 mm. For contour and surface analysis, it is clear to find that the maximum lap-shear fracture load can

be achieved at rotational speed (N) of {2300>N>1600} rpm with a pin diameter (d) of {2.75>N>3.75 mm} as shown in the light green region in Fig.5 (surface plot).

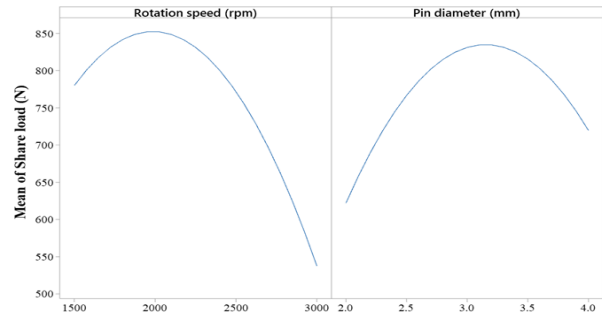


Fig. 4. Variation of the lap-shear fracture load concerning the tool speed (left) and pin diameter(right)

The resulting model was given an accepted model of R-sq and R-sq(adj) values of more than 97% and R-sq(pred) of 87.92%. Equation 3 shows the predicted regression equation for the lap-shear fracture load (LS), which depends on the rotational speed (N) and the pin diameter (d).

$$LS = -1808 + 1.156N + 965d - 0.000306N^2 - 160.2d^2 + 0.02Nd \tag{3}$$

Fig. 6-a and 6-b indicate the visual view of the joint failure after the tensile test for pin diameters 3 and 4, respectively. It indicates that the joints' area was more significant during the tool speed of 2250 rpm in both cases of 3 mm and 4 mm pin diameter. The results supported the lap-shear fracture load test, where the maximum values were achieved at this rotational speed.

Table 4. ANOVA of Lap-shear fracture load vs Rotational Speed, pin diameter during FSSW

Source	DF	Adj SS	Adj MS	F-Value	P-Value
Model	5	213886	42777.2	58.06	0.003
Linear	2	102396	51198.2	69.49	0.003
Rotation speed (rpm)	1	88088	88088.2	119.55	0.002
Pin diameter (mm)	1	14308	14308.2	19.42	0.022
Square	2	110589	55294.7	75.05	0.003
Rotation speed (rpm)*Rotation speed (rpm)	1	59283	59282.7	80.46	0.003
Pin diameter (mm)*Pin diameter (mm)	1	51307	51306.7	69.63	0.004
2-Way Interaction	1	900	900.0	1.22	0.350
Rotation speed (rpm)*Pin diameter (mm)	1	900	900.0	1.22	0.350
Error	3	2210	736.8		
Total	8	216096			

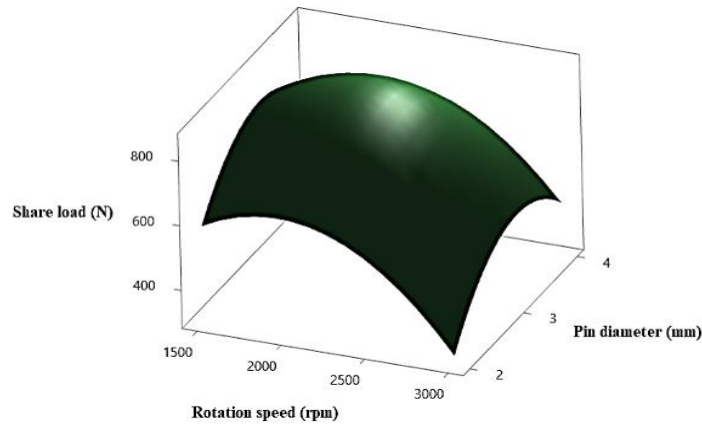


Fig. 5. lap-shear fracture load concerning FSSW parameters as a surface plot

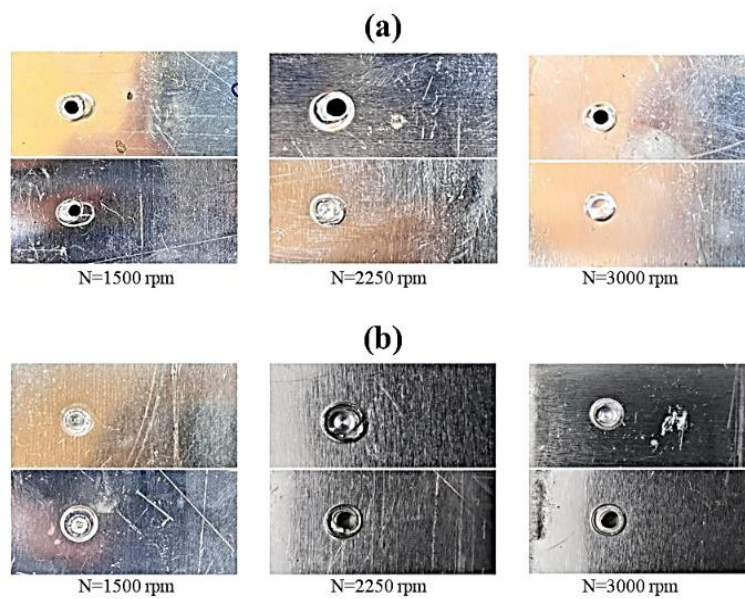


Fig. 6. Mechanical failure at a) pin d=3mm and b) pin d=4mm

The increase in rotational speed is necessary for material flow and plastic deformation of light metals in FSSW. Moreover, increasing the rotation speed increases the pin stirring action and the nugget zone [29, 30], so the nugget size is more prominent at a rotational speed of 2250 rpm than at lower speeds. When the rotational speed is higher than 2250 rpm, the metal flow will be speedy, and the plastic deformation will occur more rapidly, so the joining process will be faster, and the nugget zone will be smaller. When comparing the overall results, the rotational speed of 2250 rpm will be optimal according to the nugget size in Fig. 6-a and Fig. 6-b.

Furthermore, the behaviour of the resulting lap-shear fracture load is compatible with that obtained by [31] 40% of the results obtained by an industrial milling machine. This result is considered

encouraging and gives rise to hope for developing this work and other similar projects soon.

3.2 Hardness Profile

The Brooks hardness tester was used according to the ATSM E92-2016 standard [32] to investigate the hardness variation according to the rotational speed and pin diameter change. Fig. 7 indicates the hardness profile of the AA6061 alloy according to the change in rotational speed and pin diameter. Seven rotational speeds 1500, 1750, 2000, 2250, 2500, 2750, and 3000 rpm and two pin diameters of 3 and 4 mm were used to investigate the hardness profile using the developed FSSW apparatus. For both 3 mm and 4 mm pin diameters, it was found that the maximum hardness peak at the welding zone lies at a tool speed of 2250 rpm. The hardness value starts decreasing on both sides of the

rotational speed of 2250 in a behaviour roughly similar to that of the lap-shear fracture load delivered by the tensile test. It shows that rotational speed has a sufficient influence on the obtained

hardness values compared to the influence of the pin diameter. Even though industrial milling machines were used in previous studies [33, 34], the hardness value corresponds to what was achieved.

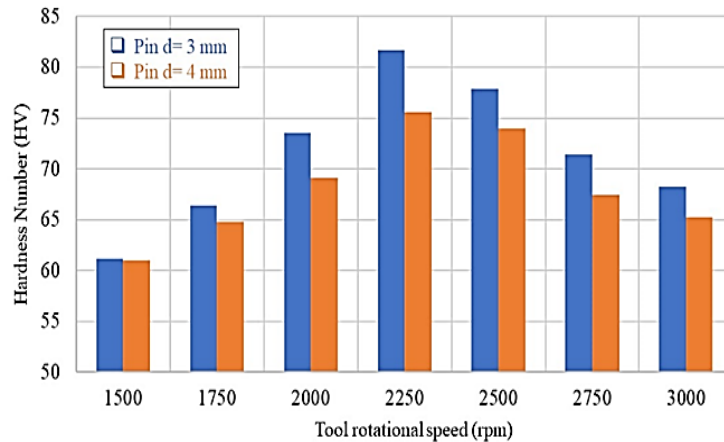


Fig. 7. FSSW Hardness profile of AA 6061 at pin d=3mm and 4mm

3.3 Bending Test

The Instron machine (Instron, USA) was used for the bending test according to the ASTM E290. The 3-point bend test can be achieved on different-sized specimens. Several critical parameters are essential, including the specimen's width, thickness, a radius of curvature, and distance between the two loading points. Three samples were tested for each rotational speed: 1750, 2250 and 2750 rpm for each pin diameter of 3 and 4mm to test 30 samples. The behaviour of the bending test has slightly deviated from the behaviour of the lap-shear fracture load and hardness profile, where a good bending test

was achieved at a pin diameter of 4 mm. All specimens at a tool speed of 2250 rpm and a pin diameter of 4 mm succeed in the test which they achieve about 180 degrees as shown in Fig. 8-a. In contrast, the behaviour of the other samples varied between failure at angles of less than 180 degrees and failure at angles of even less than 90 degrees, especially at high rotational speeds, as shown in Fig. 8-b. It can be interpreted that at high rotational speeds, the metal flow becomes more than expected, which means that part of the metal will flow outside the limits of the weld point, which leads to the weakness of the welded joint and failure.

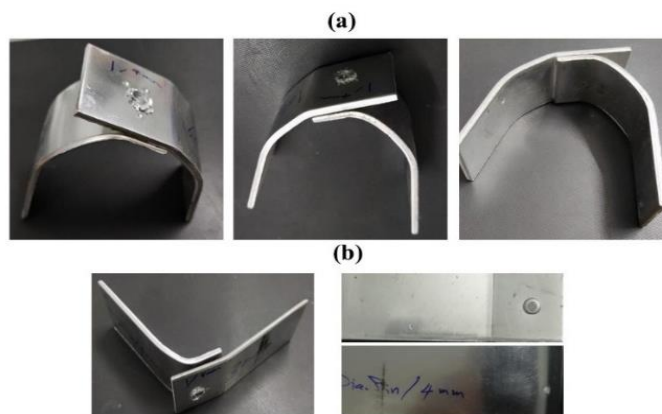


Fig. 8. Bending test specimens at (a) 2250 rpm (b) 1500 rpm

4. CONCLUSION

A portable domestic drilling machine is used to construct an FSSW apparatus. The results indicated that the joints welded by the developed apparatus have good strength and hardness. Furthermore,

most specimens are successfully bent, especially when the tool speed is set at 2250 rpm. Also, the mechanical properties improve as the pin diameter and tool speed increase. The best mechanical properties are obtained at a tool speed of 2250 rpm and a pin diameter of 3mm.

In most cases, a pin diameter of 3 mm gives the best results compared with a pin diameter of 4 mm. As a result, the portable domestic drilling machine can prepare the FSSW apparatus by replacing the regular beat tool drill with an FSSW tool with a shoulder of 10 mm, pin diameter of 3 mm and rotational speed of 2250 rpm. Finally, it was found that the dwelling time in all cases is 15 s.

As future recommendations, the suggested apparatus opens the gate for using such a tool for repairing polymers and light metals locally. Moreover, work can be modified by applying automatic axial movement of the drill instead of manual movement and measuring pressure with a load cell. Furthermore, it can be modified as a portable FSSW tool using a pneumatic rather than a regular electrical source.

REFERENCES

- [1] M.K. Kulekci, U. Esme, O. Er, Experimental comparison of resistance spot welding and friction-stir spot welding processes for the en aw 5005 aluminum alloy. *Materiali in Tehnologije*, 45(5), 2011: 395-399.
- [2] P. Briskham, N. Blundell, L. Han, R. Hewitt, K. Young, D. Boomer, Comparison of self-pierce riveting, resistance spot welding and spot friction Joining for aluminium automotive sheet. *SAE International*, 2006: 2006-01-0774. <https://doi.org/10.4271/2006-01-0774>
- [3] R.K. Al-Sabur, A.K. Jassim, friction stir spot welding applied to weld dissimilar metals of aa1100 al-alloy and C11000 copper. *IOP Conference Series: Materials Science and Engineering*, 455(1), 2018: 012087. <https://doi.org/10.1088/1757-899X/455/1/012087>
- [4] T.Y. Pan, Friction stir spot welding (FSSW) - A literature review. *SAE International*, 2007: 2007-01-1702. <https://doi.org/10.4271/2007-01-1702>
- [5] Z. Feng, M.L. Santella, S.A. David, M. Kuo, R.S. Bhatnagar, R.J. Steel, S.M. Packer, T. Pan, friction stir spot welding of advanced high-strength steels - a feasibility study. *SAE International*, 2005: 2005-01-1248. <https://doi.org/10.4271/2005-01-1248>
- [6] Y. Tozaki, Y. Uematsu, K. Tokaji, A newly developed tool without probe for friction stir spot welding and its performance. *Journal of Materials Processing Technology*, 210(6-7), 2010: 844-851. <https://doi.org/10.1016/j.jmatprotec.2010.01.015>
- [7] X.W. Yang, T. Fu, W.Y. Li, Friction stir spot welding: A review on joint macro - and microstructure, property, and process modelling. *Advances in Materials Science and Engineering*, 2014, 2014: 697170. <https://doi.org/10.1155/2014/697170>
- [8] R.S. Mishra, P.S. De, N. Kumar, Friction stir welding and processing: Science and engineering. *Springer Cham*, 2014. <https://doi.org/10.1007/978-3-319-07043-8>
- [9] H. Badarinarayan, Q. Yang, S. Zhu, Effect of tool geometry on static strength of friction stir spot-welded aluminum alloy, *International Journal of Machine Tools and Manufacture*, 49(2), 2009: 142-148. <https://doi.org/10.1016/j.ijmactools.2008.09.004>
- [10] V.X. Tran, J. Pan, T. Pan, Effects of processing time on strengths and failure modes of dissimilar spot friction welds between aluminum 5754-O and 7075-T6 sheets. *Journal of Materials Processing Technology*, 209(8), 2009: 3724-3739. <https://doi.org/10.1016/j.jmatprotec.2008.08.028>
- [11] R. Al-Sabur, A.K. Jassim, E. Messele, Real-time monitoring applied to optimize friction stir spot welding joint for AA1230 Al-alloys. *Materials Today: Proceedings*, 42(5), 2021: 2018-2024. <https://doi.org/10.1016/j.matpr.2020.12.253>
- [12] M. Merzoug, M. Mazari, L. Berrahal, A. Imad, Parametric studies of the process of friction spot stir welding of aluminium 6060-T5 alloys. *Materials & Design*, 31(6), 2010: 3023-3028. <https://doi.org/10.1016/j.matdes.2009.12.029>
- [13] Z. Shen, X. Yang, Z. Zhang, L. Cui, Y. Yin, Mechanical properties and failure mechanisms of friction stir spot welds of AA 6061-T4 sheets. *Materials & Design*, 49, 2013: 181-191. <https://doi.org/10.1016/j.matdes.2013.01.066>
- [14] Y. S. Sato, M. Fujimoto, N. Abe, H. Kokawa, Friction stir spot welding phenomena in Al alloy 6061. *Materials Science Forum*, 638-642, 2010: 1243-1248. <https://doi.org/10.4028/www.scientific.net/MSF.638-642.1243>
- [15] Y.F. Sun, H. Fujii, N. Takaki, Y. Okitsu, Microstructure and mechanical properties of mild steel joints prepared by a flat friction stir spot welding technique. *Materials & Design*, 37, 2012: 384-392.

- <https://doi.org/10.1016/j.matdes.2012.01.027>
- [16] Y.C. Chiou, C. te Liu, R. T. Lee, A pinless embedded tool used in FSSW and FSW of aluminum alloy. *Journal of Materials Processing Technology*, 23(11), 2013: 1818-1824.
<https://doi.org/10.1016/j.imatprotec.2013.04.018>
- [17] C. Schmal, G. Meschut, Refill friction stir spot and resistance spot welding of aluminium joints with large total sheet thicknesses (III-1965-19). *Welding in the World*, 64(9), 2020: 1471-1480.
<https://doi.org/10.1007/s40194-020-00922-2>
- [18] X. Lyu, M. Li, X. Li, J. Chen, Double-sided friction stir spot welding of steel and aluminum alloy sheets. *The International Journal of Advanced Manufacturing Technology*, 96(5-8), 2018: 2875-2884.
<https://doi.org/10.1007/s00170-018-1710-x>
- [19] S. Gopi K. Manonmani, Predicting tensile strength of double side friction stir welded 6082-T6 aluminium alloy. *Science and Technology of Welding and Joining*, 17(7), 2013: 601-607.
<https://doi.org/10.1179/1362171812y.0000000055>
- [20] A.K. Pandey, S.S. Mahapatra, Investigation of weld zone obtained by friction stir spot welding (FSSW) of aluminium-6061 alloy. *Materials Today: Proceedings*, 18(7), 2019: 4491-4500.
<https://doi.org/10.1016/j.matpr.2019.07.419>
- [21] S.R. Yazdi, B. Beidokhti, M. Haddad-Sabzevar, Pinless tool for FSSW of AA 6061-T6 aluminum alloy. *Journal of Materials Processing Technology*, 267 2019: 44-51.
<https://doi.org/10.1016/j.imatprotec.2018.12.005>
- [22] S. Alaeibehmand, S.E. Mirsalehi, E. Ranjbarnodeh, Pinless FSSW of DP600/Zn/AA6061 dissimilar joints. *Journal of Materials Research and Technology*, 15, 2021: 996-1006.
<https://doi.org/10.1016/j.jmrt.2021.08.071>
- [23] R. Al-Sabur, Tensile strength prediction of aluminium alloys welded by FSW using response surface methodology - Comparative review. *Materials Today: Proceedings*, vol. 45(6), 2021: 4504-4510.
<https://doi.org/10.1016/j.matpr.2020.12.1001>
- [24] K.Mahalik, J.N. Sahu, A. v. Patwardhan, B.C. Meikap, Statistical modelling and optimization of hydrolysis of urea to generate ammonia for flue gas conditioning. *Journal of Hazardous Materials*, 182(1-3), 2010: 603-610.
<https://doi.org/10.1016/j.jhazmat.2010.06.075>
- [25] S.K. Behera, H. Meena, S. Chakraborty, B. C. Meikap, Application of response surface methodology (RSM) for optimization of leaching parameters for ash reduction from low-grade coal. *International Journal of Mining Science and Technology*, 28(4), 2018: 621-629.
<https://doi.org/10.1016/j.ijmst.2018.04.014>
- [26] R. Al-Sabur, H.I. Khalaf, A. Świerczyńska, G. Rogalski, H.A. Derazkola, Effects of noncontact shoulder tool velocities on friction stir joining of polyamide 6 (PA6). *Materials*, 15(12), 2022: 4214.
<https://doi.org/10.3390/ma15124214>
- [27] H.I. Khalaf, R. Al-sabur, M.E. Abdullah, A. Kubit, H.A. Derazkola, Effects of underwater friction stir welding heat generation on residual stress of AA6068-T6 aluminum alloy. *Materials*, 15(6), 2022: 2223.
<https://doi.org/10.3390/ma15062223>
- [28] P. Vivek, D.B. Jeroen, H. Henrik, I. Mattias, A. Saeed, A. Joel, S. Jörgen, High-speed friction stir welding in light weight battery trays for the EV industry. *Science and Technology of Welding and Joining*, 27(4), 2022: 250-255.
<https://doi.org/10.1080/13621718.2022.2045121>
- [29] P. Xue, G.M. Xie, B.L. Xiao, Z.Y. Ma, L. Geng, Effect of heat input conditions on microstructure and mechanical properties of friction-stir-welded pure copper. *Metallurgical and Materials Transactions A*, 41(8), 2010: 2010-2021.
<https://doi.org/10.1007/s11661-010-0254-y>
- [30] M. Jabbari, C.C. Tutum, Optimum rotation speed for the friction stir welding of pure copper. *ISRN Materials Science*, 2013, 2013: 978031.
<https://doi.org/10.1155/2013/978031>
- [31] M.A. Tashkandi, J.A. Al-jarrah, M. Ibrahim, Spot welding of 6061 aluminum alloy by friction stir spot welding process. *Engineering, Technology & Applied Science Research*, 7(3), 2017, 1629-1632.
<https://doi.org/10.48084/etasr.1125>
- [32] Standard Test Methods for Vickers Hardness and Knoop Hardness of Metallic Materials. *ASTM International*, E92-16, 2017: 1-27.
- [33] A. Mohamad Hanapiah, S. Islam, N. Khandoker, M. Abdul Md, Shear and hardness properties study of aa-6061 aluminium alloy lap-joints

produced by friction stir spot welding process using H13 tool steel. *International Journal of Engineering Materials and Manufacture*, 6(3), 2021: 187-194.

<https://doi.org/10.26776/ijemm.06.03.2021.10>

- [34] G. Lakshmi Balasubramaniam, E, Boldsaikhan, G.F. Joseph Rosario, S.P. Ravichandran, S.

Fukada, M. Fujimoto, K. Kamimuki, Mechanical properties and failure mechanisms of refill friction stir spot welds. *Journal of Manufacturing and Materials Processing*, 5(4), 2021: 118.

<https://doi.org/10.3390/jmmp5040118>